Additive Manufacturing 9 (2016) 1–6

Contents lists available at ScienceDirect

Additive Manufacturing

journal homepage: www.elsevier.com/locate/addma

Single scan vector prediction in selective laser melting

Wessel W. Wits[a,*], Rutger Bruins[b], Lennard Terpstra[a], Rob A. Huls[b], H.J.M. Geijselaers[a]

[a] Faculty of Engineering Technology, University of Twente, P.O. Box 217, Enschede, The Netherlands
[b] National Aerospace Laboratory NLR, P.O. Box 153, Emmeloord, The Netherlands

ARTICLE INFO

Article history:
Received 27 April 2015
Received in revised form 26 August 2015
Accepted 14 December 2015
Available online 19 December 2015

Keywords:
Additive manufacturing
Selective laser melting (SLM)
Process control
Predictive modeling
Scan vector melting

ABSTRACT

In selective laser melting (SLM) products are built by melting layers of metal powder successively. Optimal process parameters are usually obtained by scanning single vectors and subsequently determining which settings lead to a good compromise between product density and build speed. This paper proposes a model that describes the effects occurring when scanning single vectors. Energy absorption and heat conduction are modeled to determine the temperature distribution and melt pool characteristics for different laser powers, scan speeds and layer thicknesses. The model shows good agreement with experimentally obtained scan vectors and can therefore be used to predict SLM process parameters.

1. Introduction

The selective laser melting (SLM) process builds products by melting successive layers of metal powder and is therefore classified as an Additive Manufacturing (AM) process. SLM is forecasted to partially replace conventional manufacturing processes for high-tech engineered products with its capability to manufacture high-value, low-volume, (near) net-shape parts [1].

Two important challenges in SLM production are part distortion by thermal stresses, and obtaining good and reproducible part properties [2]. The main focus of this paper is on the latter. However, the results of this study will also be used as input for methods treating the former (residual stress prediction). The properties of SLM manufactured parts strongly depend on the quality of each single laser-melted track. Moreover, obtaining uniform tracks well attached to the substrate or previous layer is a necessary requirement for the fabrication of high-quality parts [3]. Kruth et al. [4] reported that for this a good compromise between wetting, remelting, solidification and powder bed characteristics is essential.

The SLM process is characterized by a large number of parameters such as laser power, scan speed, spot size, scan line spacing (hatch distance), thickness of the powder layer, scanning strategy, working atmosphere, temperature of powder bed, and material properties. All of these parameters have an effect on the track formation. Unfortunately, their mutual interaction is not always clear [5].

This paper addresses the prediction of single laser-melted tracks (i.e. the scan vector or straight line that the laser converts into a solid track) in order to find the optimal process settings. The quality of single tracks depends on a limited set of the aforementioned process parameters. The most important process parameters for the production of single tracks are the laser power, scan speed, laser spot size and the thickness of the deposited powder layer. Suitable ranges of process parameter values for optimal mechanical properties or minimal process time can be obtained experimentally by producing short tracks using many single scan vectors and examining the influence of each parameter change. This is however very time consuming and costly, especially considering the potential number of new materials and powders. Experimentation only also does not yield the necessary insights into the physical processes behind the results.

Therefore in this study a numerical model is developed and validated experimentally. The model can predict the resulting track width and attachment of single scan vectors based on the mentioned process parameters. The model improves process knowledge insight and reduces the cost of predicting parameter ranges for which single scan vectors are of good quality.

2. Numerical modeling

To predict the behavior of the laser melting and solidification of a single scan vector, this process is modeled in a finite element code. Due to the scan vector symmetry, a half symmetrical model is

* Corresponding author.
E-mail address: w.w.wits@utwente.nl (W.W. Wits).

http://dx.doi.org/10.1016/j.addma.2015.12.001
2214-8604/

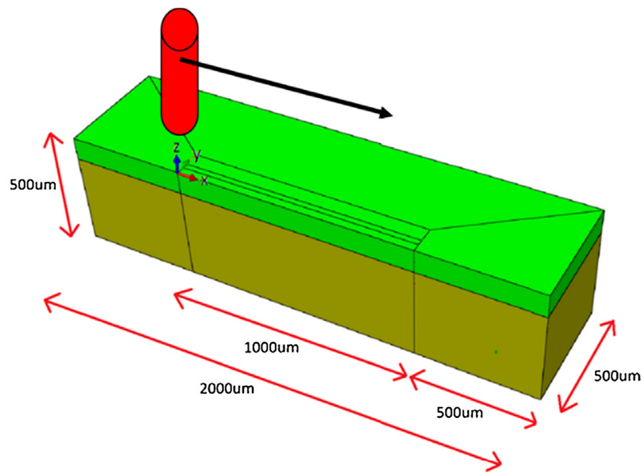

Fig. 1. Single scan vector model geometry (half symmetrical).

built (Fig. 1). The metal powder bed is modeled as a homogenized powder layer on top of a solid substrate of the same material (i.e. the layer of material that was previously deposited). The length of the model in the direction in which the laser is moving is 2 mm, the thickness is 0.5 mm (5× the powder bed layer thickness) and the width is also 0.5 mm (approx. 14× the laser spot size radius), as shown in Fig. 1. A track length of 1 mm is scanned. The dimensions are chosen such that a quasi-steady melt pool behavior is achieved for the parameter ranges of interest. Depositing multiple layers in the model is considered unnecessary, because scanning an entire layer in the experiments (described later) and then depositing a new powder layer takes sufficient time for the deposited layer to cool down to the preheat temperature.

The laser is modeled as a constant moving heat source using the Abaqus subroutine DFLUX. To minimize output fluctuations a minimum of four elements fit within the laser spot size. The numerical model is computed in Abaqus using an implicit backwards difference algorithm with a mesh of more than 10,000 nodes.

According to Gusarov et al. [6] heat transfer by radiation and convection is small compared to heat transfer by conduction due to the large temperature gradients. Also in this study the radiative and convective heat losses at the surface were found to be irrelevant compared to the heat fluxes due to diffusion.

The initial preheating temperature is set to 453 K using a '*initial conditions' card. The temperature at the bottom interface of the model is kept constant at this temperature using a *boundary card to avoid heat accumulation. The boundary is located far enough from the melt pool to have a small influence on the temperature in the melt pool itself, which is the main interest of this paper. Thermal gradient driven mass flow in the melt pool is not considered in this work. Also, capillary instability of the melt pool is irrelevant for the selected process parameter ranges based on the Plateau–Rayleigh analysis [7].

2.1. Powder bed laser energy absorption

The laser energy absorption in the powder bed follows the description of Gusarov and Smurov [8] using slow consolidation, in which the powder bed is modeled as a packed bed of monodispersed opaque spheres. The powder bed acts as an optical medium for which the absorption of the laser energy is modeled using an effective extinction coefficient:

$$\beta = \frac{3(1-f)}{2fd_p} \tag{1}$$

Table 1
Powder bed properties relevant for the heat absorption.

Property	Symbol	Value
Mean particle diameter	d_p	33 μm
Powder layer porosity	f	0.5
Reflectivity of the material	ω	0.64
Local powder layer thickness	z_{bed}	100 μm

Here, f is the powder bed porosity and d_p is the average powder particle diameter. The relative thickness of a powder bed with thickness z_{bed} is described by the optical layer thickness:

$$\tau_L = \beta z_{bed} \tag{2}$$

The powder bed absorbs part of the laser energy. The remainder is absorbed by the solid substrate underneath. The laser energy flux per unit area absorbed by the powder bed, where the powder and substrate are of the same material, can be expressed by [9]:

$$\frac{Q}{Q_0}(0) = \frac{\omega a}{(4\omega-3)D}\{2(1-\omega^2)e^{-\tau_L} - (3+\omega e^{-2\tau_L}) \times (p_1+p_2)\} - \frac{3(1-\omega)(1-\omega e^{-2\tau_L})}{4\omega-3} \tag{3}$$

In which:

$$a = \sqrt{1-\omega} \tag{4}$$

$$D = (1-a)p_2 - (1+a)p_1 \tag{5}$$

$$p_1 = [1+a-\omega(1-a)]e^{2a\tau_L} \tag{6}$$

$$p_2 = [1-a-\omega(1+a)]e^{-2a\tau_L} \tag{7}$$

Here, Q_0 is the uniform incident surface heat flux of the laser spot and ω is the reflectivity of the specular reflection. A significant part of the incident laser energy is absorbed by the powder layer. The remaining part of the laser energy that is absorbed by the solid substrate is described by:

$$\frac{Q}{Q_0}(\tau_L) = \frac{\omega a}{(4\omega-3)D}\{(1-\omega^2)e^{-\tau_L}[(1-a)e^{-2a\tau_L} + (1+a)e^{2a\tau_L}] - 2(1-\omega)(3+\omega e^{-2\tau_L})\} - \frac{3(1-\omega)(1-\omega)e^{-\tau_L}}{4\omega-3} \tag{8}$$

The energy absorption is modeled as a volumetric heat input applied to the volume underneath the laser spot. The properties of the powder are given in Table 1.

To model the irradiated laser energy, a second order Gaussian beam shape profile is applied with a beam factor of two, associated with a laser intensity in the spot center of twice the average intensity. Fig. 2 shows the penetration profile of the laser beam for a 200 W laser power and a laser spot size of 70 μm. The z-direction indicates the penetration depth, whereas the x-axis is the axial coordinate.

2.2. Material properties

The material applied is titanium alloy Ti6Al4V. The material properties required are the thermal conductivity, heat capacity and density for both the substrate and the powder. The substrate properties were taken from Mills [10] and are listed in Table 2. For Ti6Al4V the transition from the solid (powder) phase to the liquid phase occurs between the solidus temperature (1878 K) and the liquidus temperature (1933 K). The boiling temperature is 3315 K.

The conductivity of the powder bed is mostly determined by the voids and not so much by the properties of the material [6]. For a powder bed porosity of 50% the conductivity of the powder bed is approx. 10× the conductivity of the gas in the powder bed.